APPLICATION OF METABOLOMICS BASED ON DIRECT MASS SPECTROMETRY ANALYSIS FOR THE ELUCIDATION OF ALTERED METABOLIC PATHWAYS IN SERUM FROM THE APP/PS1 TRANSGENIC MODEL OF ALZHEIMER'S DISEASE

Raúl González-Domínguez[a,b,c], Tamara García-Barrera[a,b,c*], Javier Vitorica[d,e,f], José Luis Gómez-Ariza[a,b,c*]

[a]Department of Chemistry and CC.MM. Faculty of Experimental Sciences. University of Huelva. Campus de El Carmen. 21007 Huelva. SPAIN; [b]Campus of Excellence International ceiA3. University of Huelva. SPAIN; [c]Research Center of Health and Environment (CYSMA). University of Huelva. Campus de El Carmen. 21007 Huelva. SPAIN; [d]Department Bioquímica, Bromatologia, Toxicología y Medicina Legal, Faculty of Pharmacy, University of Seville. 41012 Seville. SPAIN, [e]Centro de Investigación Biomédica en Red sobre Enfermedades Neurodegenerativas (CIBERNED). 41013 Seville. SPAIN, [f]Instituto de Biomedicina de Sevilla (IBiS)–Hospital Universitario Virgen del Rocío/CSIC/University of Seville. 41013 Seville. SPAIN

Corresponding authors:
Prof. J.L Gómez Ariza, Tel.: +34 959 219968, fax: +34 959 219942, e-mail: ariza@uhu.es
Dr. T. Garcia-Barrera, Tel.: +34 959 219962, fax: +34 959 219942, e-mail: tamara@dqcm.uhu.es

ABSTRACT

Metabolomic analysis of brain tissue from transgenic mouse models of Alzheimer's disease has demonstrated a great potential for the study of pathological mechanisms and the development of new therapies and biomarkers for diagnosis. However, in order to translate these investigations to the clinical practice it is necessary to corroborate these findings in peripheral samples. To this end, this work considers the application of a novel metabolomic platform based on the combination of a two-steps extraction procedure with complementary analysis by direct infusion electrospray mass spectrometry and flow infusion atmospheric pressure photoionization mass spectrometry for a holistic investigation of metabolic abnormalities in serum samples from APP/PS1 mice. A number of metabolites were found to be perturbed in this mouse model, including increased levels of di- and tri-acylglycerols, eicosanoids, inosine, choline and glycerophosphoethanolamine; reduced content of cholesteryl esters, free fatty acids, lysophosphocholines, amino acids, energy-related metabolites, phosphoethanolamine and urea, as well as abnormal distribution of phosphocholines depending on the fatty acid linked to the molecular moiety. This allowed the elucidation of possible pathways disturbed underlying to disease (abnormal homeostasis of phospholipids leading to membrane breakdown, energy-related failures, hyperammonemia and hyperlipidemia, among others), thus demonstrating the utility of peripheral samples to investigate pathology in the APP/PS1 model.

KEYWORDS. Metabolomics, APP/PS1 mice, DI-ESI-MS, FI-APPI-MS, Alzheimer's disease

ABBREVIATIONS. AD: Alzheimer's disease; TG: transgenic; WT: wild type; QC: quality control; DI-ESI-MS: direct infusion electrospray mass spectrometry; FI-APPI-MS: flow infusion atmospheric pressure photoionization mass spectrometry; PCA: principal component analysis; PLS-DA: partial least squres discriminant analysis; VIP: variable importance in the projection; ROC: receiver operating characteristic analysis; AUC: area under the curve; CV: coefficient of variation; PE: phosphoethanolamine; GPE: glycerophosphoethanolamine; HEPE: hydroxy-eicosapentaenoic acid; PG: prostaglandin; LTB4: leukotriene B4; LPC: lyso-phosphocholine; PC: phosphocholine; DAG: diacylglycerol; CE: cholesteryl ester; TAG: triacylglycerol.

1. INTRODUCTION

Animal models are nowadays one of the most important tools in biomedical research for the investigation of disease pathophysiology, the discovery of potential biomarkers and the *in vivo* evaluation of novel therapeutic treatments [1]. The ability to create transgenic models has had a profound impact on areas such as Alzheimer's disease (AD) research, where genetics plays a prominent role. Thereby, the discovery of genes associated with pathology of this disorder, such as amyloid precursor protein (APP), presenilin 1 (PS1) and presenilin 2 (PS2) genes, has allowed the development of numerous mouse models for studying AD [2]. These models offer an outstanding opportunity to investigate the early pathological disease mechanisms, for which the application of metabolomic techniques presents a great potential. Metabolomics, defined as the comprehensive measurement of metabolites from a biological system in a high-throughput manner, allows monitoring disease perturbations because alterations in specific groups of metabolites may be sensitive to pathogenically relevant factors, reflecting changes downstream of genomic, transcriptomic and proteomic fluctuations. Furthermore, since metabolic pathways are conserved through evolution, and are essentially similar in rodents and humans, the metabolic signatures identified in AD mouse models could be directly translated into human studies [3]. Metabolomic analysis can be performed in a variety of easily accessible biofluids such as cerebrospinal fluid, blood or urine, thus highlighting the clinical utility of this approach. However, although numerous studies have been performed to assess the pathophysiological status of transgenic animals by postmortem analysis of brain tissue samples [4-9], the use of peripheral samples has been only scarcely considered. In this sense, Graham et al. analyzed comparatively brain and plasma samples from APP/PS1 and wild type mice using ^{1}H-NMR with the aim of discovering new AD biomarkers [10]. The statistical models built using plasma profiles were more accurate than those obtained with brain tissue, despite the smaller number of metabolites detected, demonstrating the potential of blood metabolomics for non-invasive investigation of metabolic abnormalities underlying to AD. Similarly, metabolomic profiling of brain and plasma samples from the TASTPM mice also revealed a number of metabolites perturbed in both matrices, which could be related to altered metabolic pathways previously associated with human AD [11]. Jiang et al. found significant differences in endogenous metabolites from serum of the senescence-accelerated mouse, suggesting perturbed glucose and lipid metabolism, and attenuated protective function of inosine [12]. Moreover, metabolomics has been also applied to examine changes in urinary metabolites of transgenic AD mice, demonstrating the utility of a very simple and easily available sample in clinical laboratory as is urine for the search of potential biomarkers [13-15].

In this work we applied a novel metabolomic multi-platform based on direct mass spectrometry analysis for the characterization of metabolic abnormalities in serum from the APP/PS1 transgenic mice. These fingerprinting tools, based on direct introduction of sample extracts containing whole metabolites into the mass spectrometer, avoid the conventional time-resolved detection of metabolites after chromatographic or electrophoretic separation, improving analysis rapidity and reproducibility, non-targeted metabolite coverage and consequently, high-throughput screening capability [16]. Furthermore, the availability of complementary atmospheric pressure ionization sources may help to delve into the high physico-chemical complexity of the metabolome. Thus, the metabolomic approach used here comprises a multistage extraction procedure for releasing a broad range of metabolites from serum samples, combined with MS analysis in positive and negative ionization modes and the complementary use of electrospray (ESI) and atmospheric pressure photoionization (APPI). Direct infusion electrospray mass spectrometry (DI-ESI-MS) has proved to be a suitable tool for fast and comprehensive "first pass" screening of metabolic abnormalities, which has been successfully applied to AD research in previous investigations using human serum [17-19] and brain tissue from transgenic mice [5,6,9]. On the other hand, González-Domínguez et al. described in a recent work that flow injection atmospheric pressure photoionization mass spectrometry (FI-APPI-MS) may complement ESI-MS for the analysis of little polar or non-polar metabolites, and it is able to differentiate serum samples from AD patients and healthy control subjects [20]. Therefore, we hypothesized that the application of this high-throughput approach combining complementary ionization techniques to the APP/PS1 mice could provide a profound understanding about metabolic alterations detectable in a peripheral sample as is blood serum, which is of great interest to allow the study of disease pathology in a non-invasive manner and for the discovery of reliable biomarkers.

2. MATERIALS AND METHODS

2.1. ANIMAL HANDLING

Transgenic APP/PS1 mice (C57BL/6 background) were generated as previously described by Jankowsky et al., expressing the Swedish mutation of APP together with PS1 deleted in exon 9 [21]. On the other hand, age-matched wild-type mice of the same genetic background (C57BL/6) were purchased from Charles River Laboratory for their use as controls. In this study, male and female animals at 6 months of age were used for experiments (TG: N=30, male/female 13/17; WT: N=30, male/female 15/15). Animals were acclimated for 3 days after reception in rooms with a 12-h light/dark cycle at 20-25 °C, with water and food available *ad libitum*. Then, mice were anesthetized by isoflurane inhalation and blood was extracted by cardiac puncture. Blood samples were immediately cooled in fridge and protected from light for 30 minutes to allow clot retraction, and then centrifuged at 1500×g for 10 minutes at 4ºC. Serum was aliquoted in Eppendorf tubes and frozen at -80°C until analysis. Animals were handled according to the directive 2010/63/EU stipulated by the European Community, and the study was approved by the Ethical Committee of University of Huelva.

2.2. SERUM PREPARATION

Serum samples were extracted following a two-stage sequential procedure described elsewhere [18]. For this, 100 µL of serum were mixed with 400 µL of methanol/ethanol (1:1, v/v) and stirred for 5 min, followed by centrifugation at 2000×g for 10 min at 4°C. The supernatant was transferred to another tube, and the precipitate was kept for further treatment. Then, supernatant was dried under nitrogen stream and the resulting residue reconstituted with methanol/water (80:20, v/v) containing 0.1% formic acid (aqueous extract). On the other hand, the precipitate isolated in the first step was extracted with 400 µL of chloroform:methanol (1:1, v/v) by stirring during 5 min, followed by centrifugation at 13000×g for 10 minutes at 4 °C. Finally, the resulting supernatant was taken to dryness under nitrogen stream and reconstituted with 100 microliters of dichloromethane:methanol (60:40, v/v) containing 10 mM ammonium formate (organic extract). Furthermore, quality control (QC) samples were prepared by pooling equal volumes of each sample and analyzed throughout the sequence run, which allows monitoring instrumental drifts along the analysis period [22]. Samples were randomized before analysis, and QC samples were injected every 10 individual serum samples.

2.3. METABOLOMIC ANALYSIS

Mass spectrometry experiments were performed in a quadrupole-time-of-flight mass spectrometer, model QSTAR XL Hybrid system (Applied Biosystems, Foster City, CA, USA), using the electrospray (ESI) and atmospheric pressure photoionization (APPI) sources according to the methods previously optimized by González-Domíguez et al. [18,20]. For accurate mass measurement, the TOF analyzer was calibrated before analyzing each batch of samples using renin and taurocholic acid as standards (in positive and negative modes, respectively).

2.3.1. METABOLOMIC ANALYSIS BY DI-ESI-MS

Samples were introduced into the mass spectrometer at 5 µL min^{-1} flow rate using an integrated apparatus pump and a 1000 µL volume Hamilton syringe. Data were obtained in both positive and negative ionization modes, acquiring full scan spectra for 0.2 minutes in the m/z range 50-1100 with 1.005 seconds scan time. In positive mode, the ion spray voltage (IS) was set at 3300 V, and high-purity nitrogen was used as curtain and nebulizer gas at flow rates about 1.13 L min^{-1} and 1.56 L min^{-1}, respectively. The source temperature was fixed at 60ºC, with a declustering potential (DP) of 60 V and a focusing potential (FP) of 250 V. For ESI(-) only few parameters were modified respect ESI(+) method, with an ion spray voltage at -4000 V, a declustering potential (DP) of -100 V and a focusing potential (FP) of -250 V. To acquire MS/MS spectra, nitrogen was used as collision gas.

2.3.2. METABOLOMIC ANALYSIS BY FI-APPI-MS

For FI-APPI analysis, serum samples were introduced by flow injection using an Accela LC system (Thermo Fisher Scientific) equipped with autosampler and quaternary pump. In addition, a model KDS 100 syringe pump from KD scientific (New Hope, PA, USA) was employed to deliver the dopant for photospray ionization. Methanol was used as flow injection solvent at 50/100 µl min^{-1}, in positive and negative ion mode respectively, while toluene (dopant) was delivered at 20/40 µl min^{-1}, in both ionization modes. Data were obtained both in positive and negative ion modes, injecting 10 µl of sample, and acquiring full scan spectra in the m/z range 50-1100 with 1.005 seconds of scan time. The ion spray voltage (IS) was set at 1500 V and -2300 V in positive and negative modes respectively, with declustering potential (DP) of ±50 V and focusing potential (FP) of ±250 V. The source temperature was maintained at 400ºC, and the gas flows (high-purity nitrogen) were fixed at 1.13 L min^{-1} for curtain gas, 1.50 L min^{-1} for nebulizer gas, 3.0 L min^{-1} for heater gas, and 1 L min^{-1} for lamp gas. To acquire MS/MS spectra, nitrogen was used as collision gas.

2.4. DATA ANALYSIS

Metabolomic data were submitted to peak detection by Markerview™ software (Applied Biosystems) in order to filter the mass spectrometry results, and to carry out the reduction into a two-dimensional data matrix of spectral peaks and their intensities. For this, all peaks above the noise level (10 counts, determined empirically from experimental spectra) were selected and binned in intervals of 0.1Da. Finally, data were normalized according to the total area sum. Then, data were subjected to multivariate analysis by partial least squares discriminant analysis (PLS-DA) in order to compare metabolomic profiles obtained, using the SIMCA-P™ software (version 11.5, UMetrics AB, Umeå, Sweden). Before performing statistical analysis, data are usually scaled and transformed in order to minimize the technical variability between individual samples to extract the relevant biological information from these data sets [23]. For this, data was submitted to Pareto scaling, for reducing the relative importance of larger values, and logarithmic transformation, in order to approximate a normal distribution. Quality of the models was assessed by the R^2 and Q^2 values, supplied by the software, which provide information about the class separation and predictive power of the model, respectively. These parameters are ranged between 0 and 1, and they indicate the variance explained by the model for all the data analyzed (R^2) and this variance in a test set by cross-validation (Q^2). Finally, potential biomarkers were selected according to the Variable Importance in the Projection (VIP: a weighted sum of squares of the PLS weight, which indicates the importance of the variable in the model) with confidence intervals derived from jack-knifing. Only variables with VIP values higher than 1.5 were considered, indicative of significant differences among groups. These metabolites were validated by t-test with Bonferroni correction for multiple testing (p-values below 0.05), using the STATISTICA 8.0 software (StatSoft, Tulsa, USA). Furthermore, the potential biomarkers were subjected to receiver operating characteristic (ROC) analysis to assess their diagnostic ability. The ROC curve analysis was performed using the GraphPad Prism software (version 6.04, Intuitive Software for Science, San Diego, CA), and the area under the curve (AUC) was used as a metric of sensitivity and specificity of these biomarkers. Thereby, a marker is excellent when AUC ranges from 0.9 to 1, good if AUC is 0.8 to 0.9, moderate if AUC is 0.8 to 0.7 and poor below 0.7 [24].

2.5. METABOLITES IDENTIFICATION

Potential biomarkers were identified matching the experimental accurate mass and tandem mass spectra (MS/MS) with those shown in metabolomic databases (HMDB, METLIN and LIPIDMAPS), and then confirmed with commercial standards when available. On the other hand, the identity of individual lipids was confirmed based on characteristic fragmentation patterns previously described. Phosphatidylcholines presented characteristic ions in positive ionization mode at m/z 184.073, 104.107 and 86.096, and two typical fragments due to the loss of trimethylamine (m/z 59) and phosphocholine (m/z 183, 205 or 221, if the counterion is proton, sodium or potassium). In contrast, a distinctive signal was found at 168.041 in negative mode [25]. Furthermore, the fragmentation in the glycerol backbone and release of the fatty acyl substituents enabled the identification of individual species of phospholipids, as previously described [26]. Fragmentation of glycerolipids (di- and tri-acylglycerols) occurs through the release of fatty acids generating different types of ions (named A, B, C and D), which show characteristic m/z values according to the fatty acid attached to the glycerol backbone [27]. On the other hand, cholesteryl esters can be easily identified by means of an abundant fragment ion at m/z 369.351 produced upon collision induced dissociation [28]. Finally, acylcarnitines [29] and eicosanoids [30] were also confirmed with characteristic fragments described in the literature

3. RESULTS AND DISCUSSION

3.1. COMPARISON OF METABOLOMIC FINGERPRINTS

A high-throughput metabolomic approach based on the combination of a two-steps extraction procedure with complementary analysis by DI-ESI-MS and FI-APPI-MS was used in this work to perform a rapid screening of serum metabolites in the APP/PS1 transgenic model. In a previous study we reported that protein precipitation with organic solvents allows the extraction of hydrophilic metabolites from serum samples, but fails to extract the lipophilic components that may remain adsorbed to protein precipitate, so that a second extraction step is necessary to recover lipid compounds [18]. Furthermore, it was demonstrated that direct analysis of these extracts by ESI/APPI-MS provides a comprehensive snapshot of serum metabolites with high sensitivity and reproducibility, and without significant matrix-based ion suppression effects [18,20]. In the present study, this procedure was applied to serum samples from transgenic APP/PS1 and wild-type mice, and metabolomic fingerprints obtained were subsequently subjected to multivariate statistics in order to evaluate the classification power of the approach. As a first exploratory step, principal component analysis (PCA) was applied for a preliminary evaluation of data quality. A good clustering of quality control samples was observed in the scores plot (Fig 1a-b, for ESI

and APPI data, respectively), indicative of stability during the analyses, without significant outliers according to the Hotelling T^2-range plot (not shown). Then, partial least squares discriminant analysis (PLS-DA) demonstrated a clear classification of APP/PS1 and control mice along the first latent variable (Fig 1c-d, for ESI and APPI data, respectively), which yielded satisfactory values for the quality parameters R^2 and Q^2, with regards to both DI-ESI-MS ($R^2 = 0.991$, $Q^2 = 0.761$) and FI-APPI-MS data ($R^2 = 0.997$, $Q^2 = 0.834$). In addition, QC samples were correctly predicted in the center of the scores plots for PLS-DA models, demonstrating the robustness of the analytical procedure [22].

3.2. IDENTIFICATION OF POTENIAL BIOMARKERS

Metabolites responsible for discrimination between APP/PS1 and control animals in PLS-DA models were identified by inspecting the corresponding loadings plots, and then were validated by t-test (p value below 0.05). These potential biomarkers are listed in Table 1 along with the experimental mass, the ionization mode used for detection (ESI or APPI, in positive or negative modes), the extract where they were found (aqueous or organic extract), the fold change (FC, calculated by dividing the mean area for peaks in the APP/PS1 group by the mean area in the control group), p-value, the area under the curve (AUC) determined by ROC analysis, and the coefficient of signal variation (CV) observed in quality control samples. From these findings it is noteworthy the utility of using complementary ionization techniques to obtain a more comprehensive characterization of serum metabolome, because while ESI-MS showed the implication of numerous polar metabolites in pathology of the APP/PS1 mice, APPI-MS mainly focuses in less polar compounds. The most notable perturbation was the increase of different eicosanoids in serum from the APP/PS1 mice, including leukotriene B4 (LTB4), hydroxy-eicosapentaenoic acid (HEPE) and prostaglandins (PG), with fold changes in the range 1.6-3.8. Other lipid compounds significantly altered were increased diacylglycerols (FC ≈ 1.4) and triacylglycerols (FC = 1.3-1.6), decreased levels of free fatty acids (FC = 0.6-0.7), lysophosphocholines (FC = 0.5-0.7) and cholesteryl esters (FC ≈ 0.8), and abnormal distribution of phosphocholines depending on the fatty acid linked to the molecular moiety. Furthermore, numerous low molecular weight metabolites were also altered in serum samples from the APP/PS1 mice, such as amino acids, catabolites of phospholipids or energy-related metabolites, among others. Then, these metabolites were subjected to receiver operating characteristic analysis in order to evaluate their potential as biomarkers for diagnosis. Most of lipids identified showed only a modest diagnostic power, with AUC values in the range 0.7-0.8, including fatty acids, di- and tri-acylglycerols, phosphocholines and cholesteryl esters. However, other metabolites stand out as strong biomarkers for AD-type disorders in the APP/PS1 model, such as lysophosphocholines, eicosanoids, urea, serine, phosphoethanolamine or tyrosine, with AUC>0.9. Finally, it is also remarkable the excellent analytical reproducibility measured in QC samples, with coefficients of variation below 10% for all metabolites identified. Therefore, it could be concluded that the metabolomic platform presented in this study shows a high potential for the comprehensive assessment of metabolic alterations in serum samples from APP/PS1 mice, which is of great utility for the search of new biomarkers and the study of pathological mechanisms underlying to these metabolic disorders, as described in the next section.

3.3. BIOLOGICAL HYPOTHESIS

Metabolic alterations detected in this study (Table 1) offer the opportunity to elucidate possible biochemical pathways affected in the APP/PS1 mice, thus allowing a better understanding about disease pathology. Furthermore, these findings demonstrate the potential of using peripheral samples such as blood serum in order to characterize AD-mechanisms, providing complementary results to those observed in brain tissue, the matrix commonly employed in previous metabolomics investigations with AD models [4-9]. It is noteworthy that serum from APP/PS1 mice showed reduced levels of different amino acids (serine, valine, threonine, pyroglutamate, histidine, tyrosine, tryptophan), which may suggest that perturbations of amino acid metabolism play a critical role in the pathogenesis of AD in this mouse model. Metabolisms of serine, valine and threonine are interrelated through the amino acid threonine, an indirect precursor of valine that connects the glycine, serine and threonine metabolism pathway to biosynthesis of branched-chain amino acids. Interestingly, Hu et al. found that levels of these three amino acids are increased in the brain of TASTPM mice [11], in agreement with other metabolomic studies performed in AD brains [4,7,9], so the reduction observed in serum samples (Table 1) could indicate an important deregulation of their transport across the blood brain barrier. In this sense we also observed a significant decrease of pyroglutamic acid levels, an essential compound for the regulation of the entry of amino acids into the brain via the γ-glutamyl cycle, whose dyshomeostasis is indicative of aberrant functioning of this metabolic process. Thereby, previous studies already reported lower levels of pyroglutamate in brain [7], CSF [31] and blood [32,33] from AD patients, corroborating results presented here. On the other hand, reduced serum histidine could point to impaired synthesis of carnosine and/or histamine, important biomolecules associated with oxidative stress [34] and failures in neurotransmission

[35] respectively, whose reduction has been previously related to AD pathogenesis [18,19,33,36]. Moreover the reduction of tryptophan and tyrosine levels, precursors of serotonin and catecholamines respectively, might denote a severe disturbance in monoaminergic neurotransmission systems, which confirm previous studies in AD subjects [37-38]. Decreased urea content (Table 1) supports a disturbed homeostasis of ammonia via the urea cycle, which may elicit deleterious effects on the central nervous system and has been closely related to AD pathology [39]. Thereby, an abnormal content of urea and related amino acids has been previously found in serum [19-20,33] and brain [8-9] of AD, accompanied by altered levels of expression in different enzymes and the corresponding genes [40]. Other studies reported an increased concentration of inosine in response to an accelerated degradation of nucleotides in brain from human patients [41] and APP/PS1 mice [9], which is finally reflected in peripheral blood as revealed our metabolomic fingerprinting platform. However, Jiang et al. surprisingly described the lack of inosine in serum from the SAMP8 mice [12], demonstrating the disparity between different existing models of AD and the need to select the correct one to mimic metabolic features detected in human AD. Finally, we also observed a significant decrease of three energy-related metabolites in serum from the APP/PS1 mice: glucose, creatine and carnitine. Lower blood levels of glucose have been reported in different transgenic models of Alzheimer's disease [10-12], denoting a profound disturbance in carbohydrate and energy metabolism. On the other hand, reduced levels of creatine could be behind impaired phosphocreatine system due to mitochondrial dysfunction, as González-Domínguez et al. described in serum from human AD patients [18,20,36]. Furthermore, the decrease of free carnitine could have important consequences in the transport of fatty acids into mitochondria for β-oxidation, which is in accordance with previous studies in brain [42], CSF [43] and serum [18,36] from AD patients.

Numerous lipid compounds were also significantly perturbed in serum from APP/PS1 mice, as can be observed in Table 1. The most notable finding was an abnormal metabolism of phospholipids, regarding altered levels of phosphocholines and lysophosphocholines, as well as other related compounds such as eicosanoids, diacylglycerols and other catabolites. Enhanced degradation of phospholipids from neural membranes has been described as a key pathological hallmark in Alzheimer's disease, whose origin seems to take place in the over-activation of phospholipases, principally phospholipase A_2 [44]. However, recent studies performed in serum samples from human AD patients also point to the implication of an altered fatty acid composition of phospholipids in this membrane destabilization process, decreasing phospholipids containing polyunsaturated fatty acids (PUFA) and increasing saturated species [18,45]. In this sense we detected a substantial decrease of different phosphocholines (PC) in serum of the APP/PS1 model, in accordance with previous studies in brain from transgenic mice of AD [46-48], demonstrating the potential of serum to reflect metabolic changes occurring in brain. Nevertheless, some individual phosphocholine-species containing stearic acid (PC-18:0/18:2 and PC-18:0/22:6) were surprisingly over-expressed in these serum samples, which has been previously described only once in brain tissue from this APP/PS1 mouse model and might suggest a profound membrane remodeling [9]. Furthermore, this abnormal serum composition of phosphocholines was accompanied by an overall decrease of lysophosphocholine (LPC) levels, which could be attributed to anabolic stimulation of lysophospholipids metabolism, in agreement with previous studies in human AD [45,49]. The production of lysophospholipids by the action of phospholipase A_2 over membrane phospholipids also leads to the liberation of free fatty acids, principally arachidonic acid, which may be easily oxidized producing eicosanoids. Thereby, the accumulation of these lipid oxidation compounds (Table 1) can be considered as a suitable marker of oxidative stress and membrane breakdown. Alternatively, there is also evidence for a role of phospholipases C and D in processes associated with degradation of phospholipids in AD, although they have been much less studied [50-51]. These enzymes hydrolyze phosphodiester bonds in the hydrophilic group of phospholipids, thus releasing diacylglycerols as final products. In this context, González-Domínguez et al. recently described the elevation of total levels of diacylglycerols in serum from AD patients as potential marker of over-activated phospholipase C/D [19-20], but this is the first time that is observed in serum from transgenic mice. To conclude, this altered metabolism of phospholipids in the APP/PS1 mice was also supported by other metabolomic changes in several low molecular weight metabolites. Choline and glycerophosphoethanolamine, catabolites resulting from degradation of phospholipids, were elevated in serum samples in accordance with numerous previous studies [18,52,53]. By contrast, phosphoethanolamine levels were decreased, as previously observed in postmortem AD brains [54], corroborating the evidence for a membrane defect in Alzheimer disease.

Besides the abovementioned changes, abnormalities in lipid metabolism were also reflected in other compounds not directly related to membrane destabilization processes, including free fatty acids, cholesteryl esters and triacylglycerols. Lower levels of myristic and palmitoleic acid were found in serum from the APP/PS1 mice, in agreement with previous investigations in blood from AD patients [32,55].

However, although it is well known that polyunsaturated fatty acids are closely involved in pathogenesis of AD since they are highly concentrated in neural membranes, the role of fatty acids detected in the present work has not been elucidated. On the other hand, decreased serum content of cholesteryl esters could denote impaired cholesterol metabolism, corroborating findings described by Fabelo et al. in cortex from APP/PS1 mice [56]. Finally, the accumulation of triacylglycerols suggests a severe hyperlipidemia, one of the most important vascular risk factors that have been associated with the development of AD. Thus, several studies have reported relationships between Alzheimer's disease and high levels of lipids, principally triglycerides, in both human [18] and mice blood [57].

4. CONCLUSIONS

This work describes for the first time the application of a metabolomic multi-platform based on direct mass spectrometry analysis with the aim to investigate metabolic alterations in serum from the APP/PS1 transgenic mice of Alzheimer's disease. The combination of DI-ESI-MS and FI-APPI-MS provided a comprehensive characterization of serum metabolome, thus allowing a better understanding about AD-related mechanisms in this transgenic model. Multivariate statistics revealed disturbances in numerous metabolites, which could be associated with perturbed amino acids metabolism, energy-related failures, abnormal homeostasis of membrane phospholipids leading to membrane breakdown, hyperammonemia and hyperlipidemia, or abnormal metabolism of cholesterol, among others. The most notable finding is that many of these alterations have been previously described only in brain tissue, thus demonstrating the potential of peripheral blood serum for the investigation of disease pathology in a non-invasive manner and, subsequently, the discovery of reliable biomarkers. Finally, it is also noteworthy that perturbations detected in this work showed close similarities with previous metabolomic studies in AD patients, as described in the Discussion section, reinforcing the role of APP/PS1 mice in AD research.

Acknowledgements. This work was supported by the projects CTM2012-38720-C03-01 from the Ministerio de Ciencia e Innovación and P008-FQM-3554 and P009-FQM-4659 from the Consejería de Innovación, Ciencia y Empresa (Junta de Andalucía). Raúl González Domínguez thanks the Ministerio de Educación for a predoctoral scholarship (AP2010-4278).

REFERENCES

[1] P. McGonigle, B. Ruggeri. Animal models of human disease: Challenges in enabling translation. Biochem. Pharmacol. 2014, 87, 162-171.
[2] A.M. Hall, E.D. Roberson. Mouse models of Alzheimer's disease. Brain Res. Bull. 2012, 88, 3-12.
[3] E. Trushina, M.M. Mielke. Recent advances in the application of metabolomics to Alzheimer's disease. Biochim. Biophys. Acta 2014, 1842, 1232-1239.
[4] R.M. Salek, J. Xia, A. Innes, B.C. Sweatman, R. Adalbert, S. Randle, E. McGowan, P.C. Emson, J.L. Griffin. A metabolomic study of the CRND8 transgenic mouse model of Alzheimer's disease. Neurochem. Int. 2010, 56, 937-943.
[5] S. Lin, H. Liu, B. Kanawati, L. Liu, J. Dong, M. Li, J. Huang, P. Schmitt-Kopplin, Z. Cai. Hippocampal metabolomics using ultrahigh-resolution mass spectrometry reveals neuroinflammation from Alzheimer's disease in CRND8 mice. Anal. Bioanal. Chem. 2013, 405, 5105-5117.
[6] S. Lin, B. Kanawati, L. Liu, M. Witting, M. Li, J. Huang, P. Schmitt-Kopplin, Z. Cai. Ultra high resolution mass spectrometry-based metabolic characterization reveals cerebellum as a disturbed region in two animal models. Talanta 2014, 118, 45-53.
[7] E. Trushina, E. Nemutlu, S. Zhang, T. Christensen, J. Camp, J. Mesa, A. Siddiqui, Y. Tamura, H. Sesaki, T.M. Wengenack, P.P. Dzeja, J.F. Poduslo. Defects in mitochondrial dynamics and metabolomic signatures of evolving energetic stress in mouse models of familial Alzheimer's disease. PLoS ONE 2012, 7, e32737.
[8] R. González-Domínguez, T. García-Barrera, J. Vitorica, J.L. Gómez-Ariza. Region-specific metabolic alterations in the brain of the APP/PS1 transgenic mice of Alzheimer's disease. Biochim. Biophys. Acta 2014, 1842, 2395-2402.
[9] R. González-Domínguez, T. García-Barrera, J. Vitorica, J.L. Gómez-Ariza. Metabolomic screening of regional brain alterations in the APP/PS1 transgenic mouse model of Alzheimer's disease by direct infusion mass spectrometry. J. Pharm. Biomed. Anal. 2015, 102, 425-435.
[10] S.F. Graham, C. Holscher, P. McClean, C.T. Elliott, B.D. Green. ^{1}H NMR metabolomics investigation of an Alzheimer's disease (AD) mouse model pinpoints important biochemical disturbances in brain and plasma. Metabolomics 2013, 9, 974-983.
[11] Z.P. Hu, E.R. Browne, T. Liu, T.E. Angel, P.C. Ho, E.C.Y. Chan. Metabonomic profiling of TASTPM transgenic alzheimer's disease mouse model. J. Proteome Res. 2012, 11,5903-5913.

[12] N. Jiang, X. Yan, W. Zhou, Q. Zhang, H. Chen, Y. Zhang, X. Zhang. NMR-based metabonomic investigations into the metabolic profile of the senescence-accelerated mouse. J. Proteome Res. 2008, 7, 3678-3686.
[13] K. Fukuhara, A. Ohno, Y. Ota, Y. Senoo, K. Maekawa, H. Okuda, M. Kurihara, A. Okuno, S. Niida, Y. Saito, O. Takikawa. NMR-based metabolomics of urine in a mouse model of Alzheimer's disease: identification of oxidative stress biomarkers. J. Clin. Biochem. Nutr. 2013, 52, 133-138.
[14] R. Gonzalez-Dominguez, R. Castilla-Quintero, T. Garcia-Barrera, J.L. Gomez-Ariza. Development of a metabolomic approach based on urine samples and direct infusion mass spectrometry. Anal. Biochem. 2014, 465, 20-27.
[15] J. Peng, K. Guo, J. Xia, J. Zhou, J. Yang, D. Westaway, D.S. Wishart, L. Li. Development of isotope labeling liquid chromatography mass spectrometry for mouse urine metabolomics: quantitative metabolomic study of transgenic mice related to Alzheimer's disease. J. Proteome Res. 2014, 13, 4457-4469.
[16] J. Draper, A.J. Lloyd, R. Goodacre, M. Beckmann. Flow infusion electrospray ionisation mass spectrometry for high throughput, non-targeted metabolite fingerprinting: a review. Metabolomics 2013, 9, S4-S29.
[17] R. Gonzalez-Dominguez, T. Garcia-Barrera, Gomez-Ariza JL. Metabolomic approach to Alzheimer's disease diagnosis based on mass spectrometry. Chem. Papers 2012, 66, 829-835.
[18] R. González-Domínguez, T. García-Barrera, J.L. Gómez-Ariza. Using direct infusión mass spectrometry forserum metabolomics in Alzheimer's disease. Anal. Bioanal. Chem. 2014, 406, 7137-7148.
[19] R. González-Domínguez, T. García-Barrera, J.L. Gómez-Ariza. Metabolomic study of lipids in serum for biomarker discovery in Alzheimer's disease using direct infusion mass spectrometry. J. Pharm. Biomed. Anal. 2014, 98, 321-326.
[20] R. González-Domínguez, T. Garcia-Barrera, J.L. Gomez-Ariza. Application of a novel metabolomic approach based on atmospheric pressure photoionization mass spectrometry using flow injection analysis for the study of Alzheimer's disease. Talanta 2015, 131, 480-489.
[21] J.L. Jankowsky, D.J. Fadale, J. Anderson, G.M. Xu, V. Gonzales, N.A. Jenkins, N.G. Copeland, M.K. Lee, L.H. Younkin, S.L. Wagner, S.G. Younkin, D.R. Borchelt. Mutant presenilins specifically elevate the levels of the 42 residue beta-amyloid peptide in vivo: evidence for augmentation of a 42-specific g secretase. Hum. Mol. Genet. 2004, 13, 159-170.
[22] T. Sangster, H. Major, R. Plumb, A.J. Wilson, I.D. Wilson. A pragmatic and readily implemented quality control strategy for HPLC-MS and GC-MS-based metabonomic analysis. Analyst 2006, 131, 1075-1078.
[23] R.A. van den Berg, H.C.J. Hoefsloot, J.A. Westerhuis, A.K. Smilde, M.J. van der Werf. Centering, scaling, and transformations: improving the biological information content of metabolomics data. BMC Genomics 2006, 7, 142.
[24] J. Xia, D.I. Broadhurst, M. Wilson, D.S. Wishart. Translational biomarker discovery in clinical metabolomics: an introductory tutorial. Metabolomics 2013, 9, 280-299.
[25] M. Pulfer, R.C. Murphy. Electrospray mass spectrometry of phospholipids. Mass Spectrom. Rev. 2003, 22, 332-364.
[26] C. Wang, S. Xie, J. Yang, Q. Yang, G. Xu. Structural identification of human blood phospholipids using liquid chromatography/quadrupole-linear ion trap mass spectrometry. Anal. Chim. Acta 2004, 525, 1-10.
[27] R. González-Dominguez, T. García-Barrera, J.L. Gómez-Ariza. Iberian ham typification by direct infusion electrospray and photospray ionization mass spectrometry fingerprinting. Rapid Commun. Mass Spectrom. 2012, 26, 835-844.
[28] G. Liebisch, M. Binder, R. Schifferer, T. Langmann, B. Schulz, G. Schmitz. High throughput quantification of cholesterol and cholesteryl ester by electrospray ionization tandem mass spectrometry (ESI-MS/MS). Biochim. Biophys. Acta 2006, 1761, 121-128.
[29] L. Vernez, G. Hopfgartner, M. Wenk, S. Krahenbuhl. Determination of carnitine and acylcarnitines in urine by high-performance liquid chromatography–electrospray ionization ion trap tandem mass spectrometry. J. Chromatogr. A 2003, 984, 203-213.
[30] R.C. Murphy, R.M. Barkley, K.Z. Berry, J. Hankin, K. Harrison, C. Johnson, J. Krank, A. McAnoy, C. Uhlson, S. Zarini. Electrospray ionization and tandem mass spectrometry of eicosanoids. Anal. Biochem. 2005, 346, 1-42.
[31] E. Trushina, T. Dutta, X.M.T. Persson, M.M. Mielke, R.C. Petersen. Identification of altered betabolic pathways in plasma and CSF in mild cognitive impairment and Alzheimer's disease using metabolomics. PLoS ONE 2013, 8, e63644.

[32] G. Wang, Y. Zhou, F.J. Huang, H.D. Tang, X.H. Xu, J.J. Liu, Y. Wang, Y.L. Deng, R.J. Ren, W. Xu, J.F. Ma, Y.N. Zhang, A.H. Zhao, S.D. Chen, W. Jia. Plasma metabolite profiles of Alzheimer's disease and mild cognitive impairment. J. Proteome Res. 2014, 13, 2649-2658.
[33] R. González-Domínguez, T. García-Barrera, J.L. Gómez-Ariza. Metabolite profiling for the identification of altered metabolic pathways in Alzheimer's disease. J. Pharm. Biomed. Anal. 2015, 107, 75-81.
[34] A.R. Hipkiss. Could carnosine or related structures suppress Alzheimer's disease? J. Alzheimers Dis. 2007, 11, 229-240.
[35] S. Nuutinen, P. Panula. Histamine in neurotransmission and brain diseases. Adv. Exp. Med. Biol. 2010, 709, 95-107.
[36] R. González-Domínguez, A. García, T. García-Barrera, C. Barbas, J.L. Gómez-Ariza. Metabolomic profiling of serum in the progression of Alzheimer's disease by capillary electrophoresis-mass spectrometry. Electrophoresis 2014, 35, 3321-3330.
[37] H. Tohgi, T. Abe, S. Takahashi, M. Kimura, J. Takahashi, T. Kikuchi. Concentrations of serotonin and its related substances in the cerebrospinal fluid in patients with Alzheimer type dementia. Neurosci. Lett. 1992, 141, 9-12.
[38] D. Storga, K. Vrecko, J.G.D. Birkmayer, G. Reibnegger. Monoaminergic neurotransmitters, their precursors and metabolites in brains of Alzheimer patients. Neurosci. Lett. 1996, 203, 29-32.
[39] V. Felipo, R.F. Butterworth. Neurobiology of ammonia. Prog. Neurobiol. 2002, 67, 259-279.
[40] F. Hansmannel, A. Sillaire, M.I. Kamboh, C. Lendon, F. Pasquier, D. Hannequin, G. Laumet, A. Mounier, A.M. Ayral, S.T. DeKosky, J.J. Hauw, C. Berr, D. Mann, P. Amouyel, D. Campion, J.C. Lambert. Is the urea cycle involved in Alzheimer's disease? J. Alzheimers Dis. 2010, 21, 1013-1021.
[41] N.R. McFarland, T. Burdett, C.A. Desjardins, M.P. Frosch, M.A. Schwarzschild. Postmortem brain levels of urate and precursors in Parkinson's disease and related disorders. Neurodegener. Dis. 2013, 12, 189-198.
[42] S.F. Graham, C. Holscher, B.D. Green. Metabolic signatures of human Alzheimer's disease (AD): ^{1}H NMR analysis of the polar metabolome of post-mortem brain tissue. Metabolomics 2014, 10, 744-753.
[43] C. Ibáñez, C. Simó, P.J. Martín-Álvarez, M. Kivipelto, B. Winblad, A. Cedazo-Mínguez, A. Cifuentes. Toward a predictive model of Alzheimer's disease progression using capillary electrophoresis–mass spectrometry metabolomics. Anal. Chem. 2012, 84, 8532-8540.
[44] A.A. Farooqui, W.Y. Ong, L.A. Horrocks. Biochemical aspects of neurodegeneration in human brain: involvement of neural membrane phospholipids and phospholipases A_2. Neurochem. Res. 2004, 29, 1961-1977.
[45] R. Gonzalez-Dominguez, T. Garcia-Barrera, J.L. Gomez-Ariza. Combination of metabolomic and phospholipid-profiling approaches for the study of Alzheimer's disease. J. Proteomics 2014, 104, 37-47.
[46] J.K. Yao, T.M. Wengenack, G.L. Curran, J.F. Poduslo. Reduced membrane lipids in the cortex of Alzheimer's disease transgenic mice. Neurochem. Res. 2009, 34, 102-108.
[47] X. Han, D.M. Holtzman, D.W. McKeel Jr. Plasmalogen deficiency in early Alzheimer's disease subjects and in animal models: molecular characterization using electrospray ionization mass spectrometry. J. Neurochem. 2001, 77, 1168-1180.
[48] R.B. Chan, T.G. Oliveira, E.P. Cortes, L.S. Honig, K.E. Duff, S.A. Small, M.R. Wenk, G. Shui, G. Di Paolo. Comparative lipidomic analysis of mouse and human brain with Alzheimer disease. J. Biol. Chem. 2012, 287, 2678-2688.
[49] N. Li, W. Liu, W. Li, S. Li, X. Chen, K. Bi, P. He. Plasma metabolic profiling of Alzheimer's disease by liquid chromatography/mass spectrometry. Clin. Biochem. 2010, 43, 992-997.
[50] S. Shimohama, Y. Sasaki, S. Fujimoto, S. Kamiya, T. Taniguchi, T. Takenawa, J. Kimura. Phospholipase C isoenzymes in the human brain and their changes in Alzheimer's disease. Neuroscience 1998, 82, 999-1007.
[51] J.K. Jin, N.H. Kim, Y.J. Lee, Y.S. Kim, E.K. Choi, P.B. Kozlowski, M.H. Park, H.S. Kim, D.S. Min. Phospholipase D1 is up-regulated in the mitochondrial fraction from the brains of Alzheimer's disease patients. Neurosci. Lett. 2006, 407, 263-267.
[52] W.E. Klunk, K. Panchalingam, R.J. McClure, J.A. Stanley, J.W. Pettegrew. Quantitative ^{1}H and ^{31}P MRS of PCA extracts of postmortem Alzheimer's disease brain. Neurobiol. Aging 1996, 17, 349-357.
[53] A. Walter, U. Korth, M. Hilgert, J. Hartmann, O. Weichel, M. Hilgert, K. Fassbender, A. Schmitt, J. Klein. Glycerophosphocholine is elevated in cerebrospinal fluid of Alzheimer patients. Neurobiol. Aging 2004, 25, 1299-1303.
[54] D.W. Ellison, M.F. Beal, J.B. Martin. Phosphoethanolamine and ethanolamine are decreased in Alzheimer's disease and Huntington's disease. Brain Res. 1987, 417, 389-392.

[55] D.C. Wang, C.H. Sun, L.Y. Liu, X.H. Sun, X.W. Jin, W.L. Song, X.Q. Liu, X.L. Wan. Serum fatty acid profiles using GC-MS and multivariate statistical analysis: potential biomarkers of Alzheimer's disease. Neurobiol. Aging 2012, 33, 1057-1066.
[56] N. Fabelo, V. Martín, R. Marín, G. Santpere, E. Aso, I. Ferrer, M. Díaz. Evidence for premature lipid raft aging in APP/PS1 double-transgenic mice, a model of familial Alzheimer disease. J. Neuropathol. Exp. Neurol. 2012, 71, 868-881.
[57] Y. Tajima, M. Ishikawa, K. Maekawa, M. Murayama, Y. Senoo, T. Nishimaki-Mogami, H. Nakanishi, K. Ikeda, M. Arita, R. Taguchi, A. Okuno, R. Mikawa, S. Niida, O. Takikawa, Y. Saito. Lipidomic analysis of brain tissues and plasma in a mouse model expressing mutated human amyloid precursor protein/tau for Alzheimer's disease. Lipids Health Dis. 2013, 12, 68.

Figure captions

Fig 1 Scores plots of statistical models for metabolomic data from serum samples; a: PCA for DI-ESI-MS data, b: PCA for FI-APPI-MS data, c: PLS-DA for DI-ESI-MS data, d: PLS-DA for FI-APPI-MS data. APP/PS1 mice: red dots, wild-type mice: blue diamonds, quality control samples: black squares

Table 1. Discriminant metabolites identified in serum from APP/PS1 mice

compound	mass	ionization mode	extract	fold change	p value	AUC	CV %
Low molecular weight metabolites							
urea	60.033	ESI+	A	0.34	$1.0 \cdot 10^{-6}$	0.96	7.9
choline	103.097	ESI+	A/O	1.34	$1.5 \cdot 10^{-3}$	0.74	5.9
serine	105.046	APPI+	A	0.43	$1.8 \cdot 10^{-5}$	0.92	7.5
valine	117.081	APPI-	A	0.81	$2.8 \cdot 10^{-3}$	0.72	7.8
threonine	119.062	ESI+/ESI-/APPI-	A	0.66	$3.5 \cdot 10^{-5}$	0.86	8.0
pyroglutamate	129.045	APPI+	O	0.74	$3.0 \cdot 10^{-5}$	0.82	7.9
creatine	131.071	APPI+	O	0.60	$3.5 \cdot 10^{-2}$	0.67	9.2
PE	141.022	ESI+	A/O	0.58	$1.8 \cdot 10^{-5}$	0.93	8.2
histidine	155.073	APPI+	O	0.69	$1.2 \cdot 10^{-2}$	0.76	7.0
carnitine	161.105	ESI+	O	0.77	$2.5 \cdot 10^{-3}$	0.72	5.2
glucose	180.067	ESI-/APPI+	A/O	0.64	$5.3 \cdot 10^{-5}$	0.83	5.7
tyrosine	181.076	ESI+/ESI-	A	0.56	$1.4 \cdot 10^{-5}$	0.90	6.8
tryptophan	204.087	ESI+	O	0.80	$8.3 \cdot 10^{-4}$	0.75	5.1
GPE	215.059	ESI+	A	1.79	$1.0 \cdot 10^{-6}$	0.85	6.7
inosine	268.085	ESI-	A/O	1.91	$1.7 \cdot 10^{-3}$	0.71	6.2
Free fatty acids							
myristic acid	228.214	APPI-	O	0.73	$3.7 \cdot 10^{-3}$	0.72	7.9
palmitoleic acid	254.230	ESI-/APPI-	O	0.61	$2.1 \cdot 10^{-3}$	0.74	8.4
Eicosanoids							
HEPE	318.222	ESI-	A/O	1.64	$1.0 \cdot 10^{-6}$	0.99	8.1
PG (series 2)	334.210	ESI-	A/O	2.54	$1.0 \cdot 10^{-6}$	0.95	9.5
LTB4	336.235	ESI-	A/O	3.44	$1.0 \cdot 10^{-6}$	0.99	7.9
PG (series 3)	350.211	ESI-	A/O	3.79	$2.0 \cdot 10^{-5}$	0.92	8.9
Lysophosphocholines							
LPC(16:1)	493.319	ESI+	A/O	0.73	$1.0 \cdot 10^{-6}$	0.85	12.1
LPC(16:0)	495.343	ESI+	A/O	0.55	$1.0 \cdot 10^{-6}$	0.91	5.1
LPC(18:2)	519.330	ESI+	A	0.73	$1.0 \cdot 10^{-6}$	0.95	5.0
LPC(18:1)	521.358	ESI+	A	0.56	$1.0 \cdot 10^{-6}$	0.90	9.3
LPC(20:4)	543.345	ESI+	A	0.61	$1.0 \cdot 10^{-6}$	0.92	4.9
LPC(22:6)	567.341	ESI+	A	0.59	$1.0 \cdot 10^{-6}$	0.91	5.4
Phosphocholines							
PC(16:0/16:0)	733.571	ESI+	O	0.76	$4.7 \cdot 10^{-4}$	0.79	3.6
PC(16:0/18:1)	759.585	ESI+/ESI-	A/O	0.71	$3.2 \cdot 10^{-4}$	0.81	3.7
PC(16:0/18:0)	761.598	ESI+/ESI-	A/O	0.75	$3.0 \cdot 10^{-4}$	0.78	8.4
PC(16:0/20:4)	781.562	ESI+/ESI-	A/O	0.76	$7.9 \cdot 10^{-4}$	0.74	6.7
PC(18:2/18:0)	785.599	ESI+	A	1.59	$2.0 \cdot 10^{-6}$	0.85	5.4
PC(18:1/20:4)	807.579	ESI+/ESI-	A/O	0.75	$2.2 \cdot 10^{-4}$	0.77	6.5
PC(18:0/22:6)	833.606	ESI+	A	1.78	$1.0 \cdot 10^{-6}$	0.85	7.4

Diacylglycerols							
DAG(18:3/18:2)	614.481	APPI+	O	1.41	$1.4 \cdot 10^{-2}$	0.68	8.1
DAG(18:3/18:1)	616.516	APPI+	O	1.44	$6.0 \cdot 10^{-3}$	0.71	5.6
Cholesteryl esters							
CE(16:1)	622.581	ESI+	O	0.77	$1.2 \cdot 10^{-3}$	0.76	4.7
CE(16:0)	624.595	ESI+	O	0.85	$1.6 \cdot 10^{-3}$	0.75	4.4
Triacylglycerols							
TAG(16:1/16:0/20:4)	852.742	ESI+/APPI+	O	1.29	$3.8 \cdot 10^{-2}$	0.68	5.5
TAG(16:0/16:0/20:4)	854.747	ESI+/APPI+	O	1.36	$1.5 \cdot 10^{-2}$	0.69	6.1
TAG(16:1/16:1/22:6)	874.712	APPI+	O	1.27	$4.2 \cdot 10^{-2}$	0.67	3.3
TAG(16:1/16:0/22:6)	876.739	ESI+/APPI+	O	1.44	$3.3 \cdot 10^{-3}$	0.70	3.8
TAG(16:0/16:0/22:6)	878.754	ESI+	O	1.64	$2.3 \cdot 10^{-4}$	0.77	4.3
TAG(16:0/16:0/22:5)	880.768	ESI+	O	1.40	$2.3 \cdot 10^{-4}$	0.78	5.4
TAG(16:1/18:2/22:6)	900.709	APPI+	O	1.58	$2.1 \cdot 10^{-3}$	0.71	3.8
TAG(16:0/18:2/22:6)	902.720	APPI+	O	1.43	$2.1 \cdot 10^{-3}$	0.72	5.7
TAG(18:1/22:6/22:6)	976.773	APPI+	O	1.39	$2.9 \cdot 10^{-3}$	0.71	4.2

Abbreviations: PE, phosphoethanolamine; GPE, glycerophosphoethanolamine; HEPE, hydroxy-eicosapentaenoic acid; PG, prostaglandin; LTB4, leukotriene B4; LPC, lyso-phosphocholine; PC, phosphocholine; DAG, diacylglycerol; CE, cholesteryl ester; TAG, triacylglycerol; A, aqueous extract; O, organic extract.

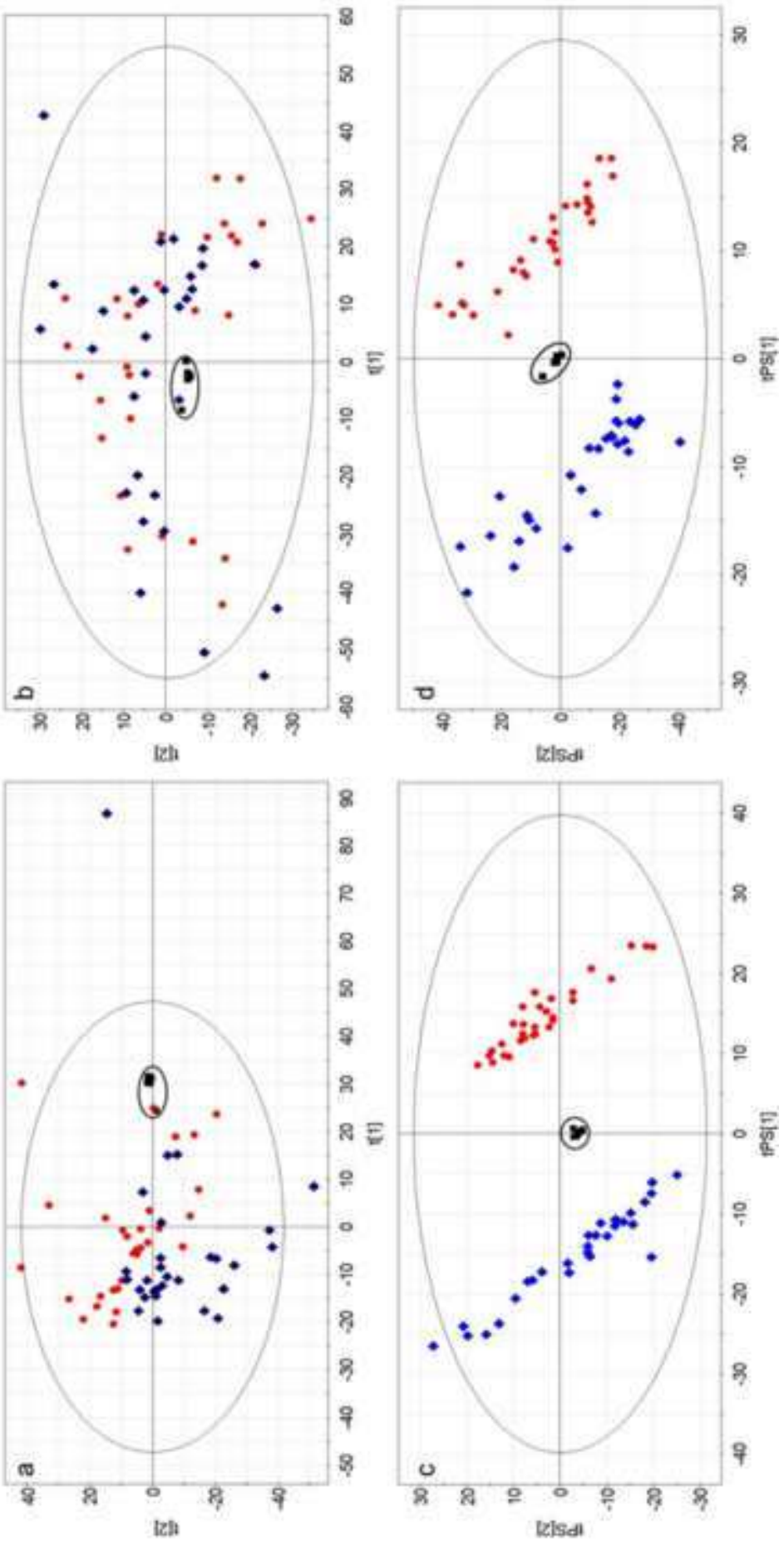

Figure 1
Click here to download high resolution image